Biomimetic membranes

DOI: 10.1002/anie.200901544

Biomimetic Lipoglycopolymer Membranes: Photochemical Surface Attachment of Supramolecular Architectures with Defined Orientation**

Stefan M. Schiller, Annette Reisinger-Friebis, Heide Götz, Craig J. Hawker, Curtis W. Frank, Renate Naumann, and W. Knoll*

Dedicated to Prof. Dr. Helmut Ringsdorf on the occasion of his 80th birthday

The assembly of defined supramolecular architectures on a molecular scale, such as biomimetic membranes,[1–3] requires the synthesis of multifunctional building blocks and a sophisticated combination of nanotechnological surface preparation techniques. A drawback of current tethered bilayer lipid membrane (tBLM) systems is their limited submembrane decoupling distance from the solid support. The necessity for large (6 nm and more) cytoplasma analogue compartments originates from several biological and biophysical requirements, such as accommodation of cytoplasmatic subunits of membrane proteins,[4] reduction of the Förster energy transfer[5] for the use of fluorescent or photoaffinity probes in vicinity of metal surfaces, and compensation for surface roughness of sensor surfaces often preventing good electrical tBLMs properties.[6] Current polymer-based tBLMs on gold do not achieve membrane–surface decoupling distances of more than 5 nm, nor are polymer based tBLMs able to maintain sufficient electrical properties (resistance of at least several $M\Omega\,cm^2$).

To overcome these limitations, we have devised a new strategy to expand the existing scope of tBLMs using lipoglycopolymers (LGP). Special emphasis was placed on increasing the cytoskeleton analogue compartment size (decoupling distance from the sensor surface) whilst retaining tightly sealing membranes, which requires the careful design of the lipid moiety, the tethering polymer, and the reactive self-assembling monolayer (SAM) to immobilize the LGP. Furthermore, we introduced a new covalent immobilization procedure that utilizes photochemical surface attachment to assemble complex supramolecular architectures of defined orientation from aqueous solution. This procedure may have interesting additional applications in the design of new protein nanoarrays and in bionanotechnology in general.

The idea of using macromolecules as a cushion[7] to mimic the cytsol/cytoskeleton of the cell to create a hydrophilic space between membrane and solid support was first introduced by Ringsdorf and Sackmann.[1,8] Macromolecular tethers impose several challenging features. They adopt coiled conformations, which strongly depend on the solvent, and have a range of molecular weights and lengths, whilst interchain interactions determine shape and stability of thin films. Lipid-functionalized small macromolecular tether systems with less than 100 repeating units n that have been used to date reached no more than 40% of their maximal theoretical thickness. Examples include poly(ethyloxazoline) ($n = 50$, length 3–3.5 nm)[9] and PEG2000 ($n = 45$, length 4.9 nm).[10] The requirements for a macromolecular tether can be summarized as follows: 1) There must be complete wetting between the surface and the hydrated polymer and between the membrane and the hydrated polymer;[11,12] 2) the interaction between membrane and surface needs to be repulsive to prevent dewetting;[37] and 3) nonspecific contacts by van der Waals attraction (effective up to about 3 nm) between lipids and surface must be suppressed.[37]

Of all known systems, the glycocalix of the cell is one of the most efficient systems to exert the functions mentioned above. The carbohydrate units of the glycocalix maintain a relatively high osmotic pressure, allowing a stable cell–cell distance between 10–100 nm and a high cooperative stabilization within the glycocalix by hydrogen bonding.[4] Therefore, a carbohydrate-modified or -based macromolecule tether can be envisioned that would enable suitable stabilization within and between tether chains. Theoretical calculations[36] show that to realize a decoupling distance of at least 6 nm, a minimum of twelve β-1,4 linked monosaccharides is required. Apart from the fact that the synthesis of dodeca-

[*] Dr. S. M. Schiller
Freiburg Institute for Advanced Studies (FRIAS), School of Soft Matter Research, Albert-Ludwigs-Universität Freiburg
Albertstrasse 19, 79104 Freiburg (Germany)
Fax: (+49) 761-203-97451
E-mail: Stefan.Schiller@FRIAS.Uni-Freiburg.de
Dr. A. Reisinger-Friebis, Dr. R. Naumann
Max Planck Institut für Polymerforschung
Ackermannweg 10, 55128 Mainz (Germany)
Dr. H. Götz
European Patent Office
Bayerstrasse 34, 80335 München (Germany)
Prof. C. J. Hawker
Department of Chemistry and Biochemistry, University of California
Santa Barbara, CA 93106-9510 (USA)
Prof. C. W. Frank
Department of Chemical Engineering, Stanford University
Stanford, California 94305-5025 (USA)
Prof. Dr. W. Knoll
Austrian Institute of Technology (AIT)
Donau-City-Strasse1, Tech Gate Vienna, 1220 Vienna (Austria)

[**] We thank Dr. Tobias Baumgart and Dr. M. Sever for helpful discussions. We are grateful to the Freiburg Institute for Advanced Studies (FRIAS), the Rektorat Uni Freiburg and the MPIP for support.

saccharides is tedious, it has been reported that glycolipids with more than four β-1,4 linked glucose monosaccharides form nonfunctional aggregates with a phase transition temperature T_m above 160 °C.[13] To circumvent these problems, we designed a novel LGP (Figure 1)[14] that is based on a

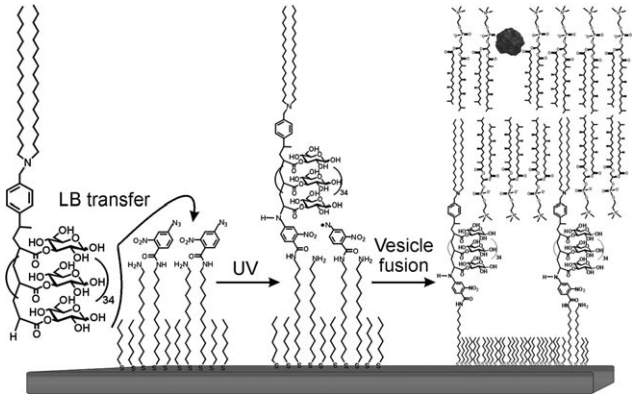

Figure 1. Photochemical attachment of preoriented lipoglycopolymers onto gold sensor surfaces after Langmuir–Blodgett (LB) transfer. Fusion of liposomes leads to the formation of tethered bilayer lipid membranes. Valinomycin, a cyclic peptide ion carrier, is used to demonstrate the functional equivalence to biological membranes.

polyacrylate backbone with β-O-3-linked glucose. One study reported a dynamic *exo*/*endo*-rotamer exchange regarding the ester–glucose–acrylate linkage, which is restricted to the *endo* rotamer in methacrylates,[15] thus allowing the acrylate side-chain carbohydrate conformational dynamics. The β-O-3-linked glucose is used because it allows the carbohydrate moiety to also be linked to the activated SAM at its reducing terminus (see below).

The lipid dioctadecylamine (DODA) was used because it forms stable LB films[16] and fluid membranes[17] with no signs of physical gelation,[16] is chemically stable at the polymerization temperature,[14] has no known signal character or protein interaction (in contrast to other lipids),[18,19] and is commercially available. It is introduced by controlled radical polymerization as the chain starting moiety of a nitriloxide initiator during D-glucose-2-propenoate polymerization.[14] The resulting polymers have a narrow polymer weight distribution of between 1.16 and 1.27. For the work presented herein, a LGP with $M_n = 9000$ (LGP9000) and a polydispersity index PDI = 1.17 was used, as LGP5900 can only theoretically extend to 5.2 nm (5 ± 1 nm achieved in practice; data not shown), and LGP15000 did not dissolve quantitatively.

As described earlier, the formation of highly defect-free tBLMs depends solely upon the dynamic interaction of the hydrophobic lipid domains.[6] A Langmuir–Blodgett trough is used to form an oriented molecular LGP film at the air–water interface. This procedure allows the alignment of the lipid groups to form an extended hydrophobic two-dimensional surface. Increasing surface pressure results in elongation of the glycopolymer chains. Langmuir–Blodgett transfer of this preorganized LGP film onto a gold surface enables the glycopolymer to adapt its length and conformation to maintain a uniform DODA layer whilst compensating for surface roughness. Furthermore, this method allows the polar glycopolymer to be linked to the substrate through the repeat unit closest to the reactive surface group, which may not be the very terminal group. This process ensures the immobilization of an elongated tether conformation whilst the lower membrane leaflet shows optimal lipid interaction.

Figure 2A compares the pressure–area isotherms of DODA and LGP9000. At high surface pressures, LGP9000 adopts an area of 58 Å^2 per molecule, which is close to the

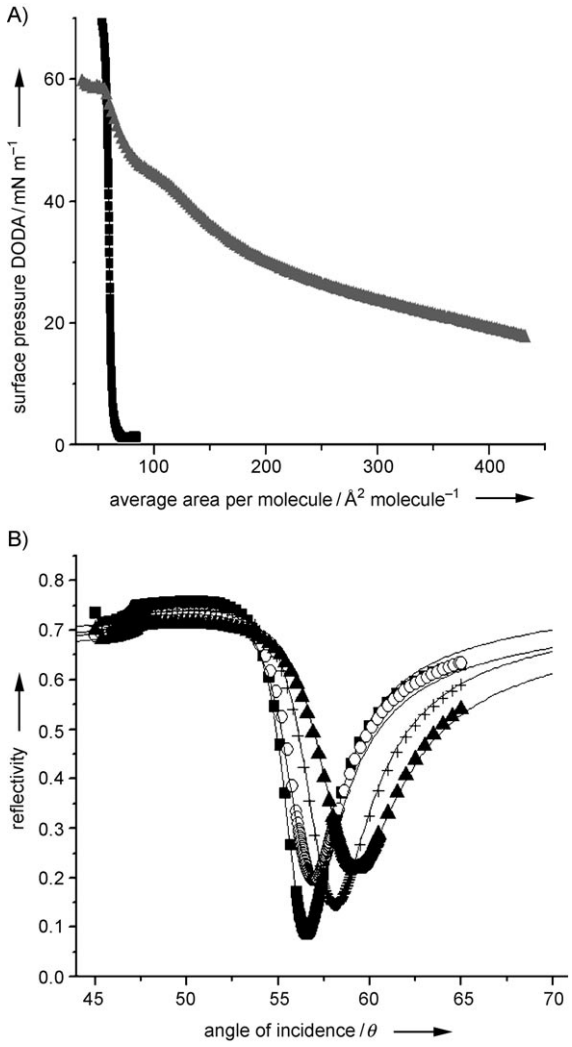

Figure 2. A) Pressure–area isotherm of DODA (■) and LGP9000 (▲) B) SPS data, Au reference (■), mixed SAM (○), mixed SAM plus ANB and LPG9000 not extracted (▲) and mixed SAM plus ANB and LPG9000, extracted(+). For values, see Table 1.

minimal area per molecules of DODA (55 Å^2). This area is large enough to accommodate the glycopolymer chain because the molecular area of a single monosaccharide unit is about 40 Å^2.[20] Because biological membranes have a surface pressure of 35 mN m^{-1},[21] the LB-transfer of the LGP was performed at 35–40 mN m^{-1}, which allows an area of 120–150 Å^2 per LGP. The transfer above the fluid condensed

phase allows an extended yet flexible glycopolymer tether, which is important to level out surface inhomogenities. Surprisingly, the LGP still reaches decoupling distances close to the theoretical maximum (Table 1), thus underlining the stabilizing effect of the carbohydrate interactions. Owing to the use of polar protic solvents to dissolve and transfer LPG, the reactive SAM can not be composed of strong electrophilic groups that are needed to bind the carbohydrates efficiently. Therefore, we use photoreactive SAMs synthesized on the surface by a two-step process. First we prepared a mixed SAM composed of 1-mercaptohexane and amino-terminated C_6- or C_{12}-spacered disulfides, which are reacted with 5-azido-2-nitrobenzoic acid chloride (ANB) to introduce the photoreactive group.

Table 1: Fit parameters of the EIS data (membrane capacitance and resistance) obtained from the spectra of Figure 3.[a]

	R_m [MΩ cm^2] experimental	A_{CPE} [F cm^{-2}]$^\alpha$	α	d [nm] experimental	d [nm] calculated
binary SAM	1.4 ± 0.5	2.0 ± 0.1	0.96	2.5 ± 0.2	2.5
azide-functionlized binary SAM	0.05 ± 0.01	8.0 ± 3	0.96	3.0 ± 0.1	3.0
lipoglycopolymer, monolayer before vesicle spreading	0.76 ± 0.1	2.7 ± 0.2	0.96	11.5 ± 1.5	12
Lipid bilayer after vesicle spreading	2.1 ± 1.0	2.5 ± 0.2	0.98	14.5 ± 2	14.5
Lipid bilayer + valinomycin + K^+	0.01 ± 0.002				

[a] A_{CPE} is the fit parameter for the CPE obtained from the ZVIEW fit routine, and α is the distribution parameter of time constants; for $\alpha = 1$, the CPE is a pure capacitor. Surface plasmon resonance data (thickness measurements d) are compared with molecule sizes obtained by modeling calculations with CS Chem3D Pro.

Mixed SAMs are used for two reasons. First, pure amino-terminated SAMs show reduced reactivity owing to in-plane interactions[22] and steric hindrance.[23] Second, they prevent a high initial resistance that would be defined by the C12-spacer and not by the membrane. 1-mercaptohexane is used as a lateral spacer to form low-order SAMs with decreased resistance. If a mixture of 1-mercaptohexane and bis(amino-hexyl) disulfide is used, the resulting photoreactive SAM is not able to covalently attach LGPs to the sensor surface. It is known that metals introduce additional electromagnetic decay channels and energy dissipation pathways,[24] causing nonradiative decay of almost 100% within 5 nm of the surface.[25] Therefore, efficient quenching has to be assumed when short chain SAMs are used. On the other hand, fluorescence is not fully quenched if the tether is longer than six methylene units, with a linear increase of fluorescence with increasing tether length.[26] We thus used a bis(aminododecyl) disulfide in combination with 1-mercaptohexane. Microphase separation of the functional amino termini is ensured by differences in alkyl chain length of five to six methylene units,[27] which is known to lead to a fine distribution of the longer chain[28] with no cluster formation.[29] This pillar-like structure allows an efficient photoactivation of ANB-terminated SAMs on gold surfaces and LGP immobilization within 5 min at wavelengths larger than 300 nm; this result is similar to conditions reported for solution experiments.[30] Figure 2B shows the surface plasmon spectroscopy (SPS) data, including irradiation experiments before and after extraction of the LGP-film with ethanol to remove noncovalently bound LGP. Within 5 min, more than 50% of the LGPs were covalently linked to the surface. ANB mainly reacts via the triplet nitrene, which is able to react with the acrylate backbone (shown for example in Figure 1) or the carbohydrate,[31] and does not show rearrangement to the didehydroazepine that would be necessary for an efficient reaction with amino groups.[31] Other experiments show the formation of an arylhydroxylamine,[32] which would allow the reaction with the reducing end of the carbohydrate moiety (alternative pathway in Figure 1).

Homogeneous vesicle fusion onto these covalently immobilized LGP monolayers using diphytanylphosphatidylcholine completed the lipid bilayer and yielded highly insulating tBLMs with large decoupling distances from the surface (Table 1). This bilayer was investigated using surface plasmon resonance spectroscopy (SPS) and electrochemical impedance spectroscopy (EIS). The impedance spectra (Figure 3A) allow the capacitance and the resistance of the lipid mono- and bilayer to be calculated by fitting the data to the equivalent circuit.[33–35]

The equivalent circuit (Figure 3B) consists of a RC mesh representing the lipid mono- or bilayer that consists of a

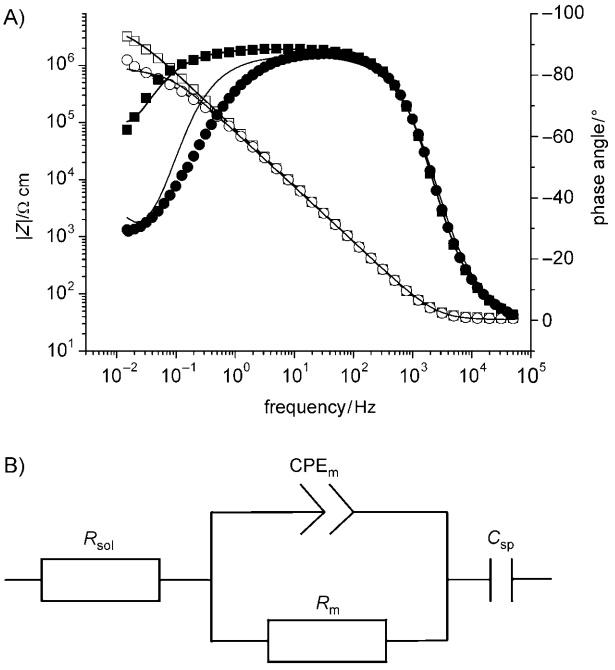

Figure 3. A) EIS analysis (Bode plot) of the LGP monolayer before (●,○) and after (□,■) vesicle fusion. The solid lines represent fitted data. Impedance Z versus frequency (□,○) and phase angle versus frequency (■,●). B) Equivalent circuit used to fit the data.

constant-phase element CPE_{mem} and resistance R_{mem} of the lipid membrane, the resistance of the electrolyte solution R_{sol}, and the capacitance of the tether C_{sp} containing the diffuse double-layer adjacent to the gold surface. The Bode plot in Figure 3 shows a significant increase in membrane resistance from the LPG monolayer to the bilayer membrane; the results are given in Table 1. Data measured for the tBLMs varied from 1 to 3 $M\Omega\,cm^2$, and single experiments achieved values over 10 $M\Omega\,cm^2$ for the resistance of the lipid membrane. These changes for very good specific resistances (above several $M\Omega\,cm^2$) can be explained by a very small difference in just a few defects over large membrane areas. The values thus compare quite well with those of the BLMs.[6] The functionality and reservoir properties of the new tBLMs were investigated using the ion carrier valinomycin; the date confirm the formation of a fluid and insulating tBLM.

In the presence of 0.1M potassium ions, a drop in resistance of up to three orders in magnitude gives rise to the so-called inflection point in the EIS spectrum that corresponds well to literature values.[6] The average decoupling distance contributed by the glycopolymer tether yielded 11.5 nm, including 3 nm for the SAM.

In conclusion, we have demonstrated the photochemical attachment of functionally oriented supramolecular architectures to gold surfaces for the first time. The resulting tBLMs achieved large decoupling distances from the solid substrate whilst maintaining electrical properties of biological membranes that are comparable to short-chain tBLMs. The superior properties of tBLMs on rough gold substrates as well can now be utilized for various applications, such as biosensor and lab-on-a-chip devices. This new approach to form lipid bilayers on polycrystalline gold surfaces eliminates the need to use labor-intense ultraflat gold substrates. Apart from traditional tBLM applications, the exceptionally large decoupling of a highly insulating layer from a sensor surface opens new avenues in molecular electronics and nanotechnology. Extension to other complex surface modifications, such as block copolymer nanoarchitectures, protein arrays, and intermolecular protein cross-linking using the photochemical attachment method on metal surfaces can now be combined with surface patterning techniques such as nano-ink-printing, stamping, and photomask techniques.

Received: March 20, 2009
Published online: August 17, 2009

Keywords: membranes · nanobiotechnology · photochemistry · polymers · supramolecular chemistry

[1] E. Sackmann, *Science* **1996**, *271*, 43 – 48.
[2] W. Knoll, I. Köper, R. Naumann, E. K. Sinner, *Electrochim. Acta* **2008**, *53*, 6680 – 6689.
[3] W. Knoll, C. W. Frank, C. Heibel, R. Naumann, A. Offenhausser, J. Ruhe, E. K. Schmidt, W. W. Shen, A. Sinner, *Rev. Mol. Biotechnol.* **2000**, *74*, 137 – 158.
[4] T. Huber, A. V. Botelho, K. Beyer, M. F. Brown, *Biophys. J.* **2004**, *86*, 2078 – 2100.
[5] I. Avrutsky, *Phys. Rev. B* **2004**, *70*, 155416.
[6] S. M. Schiller, R. Naumann, K. Lovejoy, H. Kunz, W. Knoll, *Angew. Chem.* **2003**, *115*, 219 – 222; *Angew. Chem. Int. Ed.* **2003**, *42*, 208 – 211.
[7] C. Ma, M. P. Srinivasan, A. J. Waring, R. I. Lehrer, M. L. Longo, P. Stroeve, *Colloids Surf. B* **2003**, *28*, 319 – 329.
[8] L. Haussling, W. Knoll, H. Ringsdorf, F. J. Schmitt, J. L. Yang, *Makromol. Chem. Macromol. Symp.* **1991**, *46*, 145 – 155.
[9] T. Lehmann, J. Ruhe, *Macromol. Symp.* **1999**, *142*, 1 – 12.
[10] J. C. Munro, C. W. Frank, *Langmuir* **2004**, *20*, 3339 – 3349.
[11] G. Elender, E. Sackmann, *J. Phys. II* **1994**, *4*, 455 – 479.
[12] J. Nissen, S. Gritsch, G. Wiegand, J. O. Radler, *Eur. Phys. J. B* **1999**, *10*, 335 – 344.
[13] M. Hato, H. Minamikawa, *Langmuir* **1996**, *12*, 1658 – 1665.
[14] a) H. Götz, E. Harth, S. M. Schiller, C. W. Frank, W. Knoll, C. J. Hawker, *J. Polym. Sci. Polym. Chem.* **2002**, *40*, 3379 – 3391; b) L. Y. Hwang, H. Goetz, C. J. Hawker, C. W. Frank, *Colloids Surf. B* **2007**, *54*, 127 – 135; c) L. Y. Hwang, H. Goetz, W. Knoll, C. J. Hawker, C. W. Frank, *Langmuir* **2008**, *24*, 14088 – 14098.
[15] L. Retailleau, A. Laplace, H. Fensterbank, C. Larpent, *J. Org. Chem.* **1998**, *63*, 608 – 617.
[16] C. A. Naumann, C. F. Brooks, G. G. Fuller, T. Lehmann, J. Ruhe, W. Knoll, P. Kuhn, O. Nuyken, C. W. Frank, *Langmuir* **2001**, *17*, 2801 – 2806.
[17] C. A. Naumann, O. Prucker, T. Lehmann, J. Rühe, W. Knoll, C. W. Frank, *Biomacromolecules* **2002**, *3*, 27 – 35.
[18] W. Dowhan, *Annu. Rev. Biochem.* **1997**, *66*, 199 – 232.
[19] H. Palsdottir, C. Hunte, *Biochim. Biophys. Acta Biomembr.* **2004**, *1666*, 2 – 18.
[20] K. Tamada, H. Minamikawa, M. Hato, *Langmuir* **1996**, *12*, 1666 – 1674.
[21] D. Marsh, *Biochim. Biophys. Acta Rev. Biomembr.* **1996**, 1286, 183 – 223.
[22] M. L. Wallwork, D. A. Smith, J. Zhang, J. Kirkham, C. Robinson, *Langmuir* **2001**, *17*, 1126 – 1131.
[23] T. P. Sullivan, W. T. S. Huck, *Eur. J. Org. Chem.* **2003**, 17 – 29.
[24] K. Vasilev, W. Knoll, M. Kreiter, *J. Chem. Phys.* **2004**, *120*, 3439 – 3445.
[25] J. R. Lakowicz, *Anal. Biochem.* **2001**, *298*, 1 – 24.
[26] K. W. Kittredge, M. A. Fox, J. K. Whitesell, *J. Phys. Chem. B* **2001**, *105*, 10594 – 10599.
[27] S. F. Chen, L. Y. Li, C. L Boozer, S. Y. Jiang, *Langmuir* **2000**, *16*, 9287 – 9293.
[28] S. Chen, L. Li, C. L Boozer, S. Jiang, *J. Phys. Chem. B* **2001**, *105*, 2975 – 2980.
[29] L. Li, S. Chen, S. Jiang, *Langmuir* **2003**, *19*, 3266 – 3271.
[30] C. Chambon, D. Bennat, F. Delolme, G. Dessalces, T. Blachere, M. R. de Ravel, E. Mappus, C. Grenot, C. Y. Cuilleron, *Biochemistry* **2001**, *40*, 15424 – 15435.
[31] A. Albini, G. Bettinetti, G. Minoli, *J. Chem. Soc. Perkin Trans. 2* **1999**, 2803 – 2807.
[32] T. V. Popova, V. S. Mal'shakova, P. V. Alekseyev, N. V. Kudryashova, M. M. Shakirov, L. L. Savinkova, I. A. Drachkova, T. S. Godovikova, *Nucleosides Nucleotides Nucleic Acids* **2004**, *23*, 921 – 925.
[33] C. Peggion, F. Formaggio, C. Toniolo, L. Becucci, M. R. Moncelli, R. Guidelli, *Langmuir* **2001**, *17*, 6585 – 6592.
[34] B. Raguse, V. Braach-Maksvytis, B. A. Cornell, L. G. King, P. D. Osman, R. J. Pace, L. Wieczorek, *Langmuir* **1998**, *14*, 648 – 659.
[35] G. Krishna, J. Schulte, B. A. Cornell, R. Pace, L. Wieczorek, P. D. Osman, *Langmuir* **2001**, *17*, 4858 – 4866.
[36] Calculations were carried out using CS Chem 3D Ultra (CambridgeSoft, Version 9.0).
[37] M. Tanaka, E. Sackmann, *Nature* **2005**, *437*, 656 – 663.

